IEEE Access
Multidisciplinary | Rapid Review | Open Access Journal

Received August 3, 2018, accepted September 12, 2018. Date of publication xxxx 00, 0000, date of current version xxxx 00, 0000.

Digital Object Identifier 10.1109/ACCESS.2018.2872320

Real-Time Closed-Loop Color Control of a Multi-Channel Luminaire Using Sensors Onboard a Mobile Device

SAMUEL JIA WEI TANG[1], VINEETHA KALAVALLY[1], (Member, IEEE), KOK YEW NG[1,2], (Member, IEEE), CHEE PIN TAN[3], (Senior Member, IEEE), AND JUSSI PARKKINEN[4]

[1]Electrical and Computer Systems Engineering Department, School of Engineering, Monash University Malaysia, Subang Jaya 47500, Malaysia
[2]Engineering Research Institute, Ulster University, Newtownabbey BT37 0QB, U.K.
[3]School of Engineering and Advanced Engineering Platform, Monash University Malaysia, Subang Jaya 47500, Malaysia
[4]Faculty of Science and Forestry, University of Eastern Finland, 80101 Joensuu, Finland

Corresponding author: Kok Yew Ng (mark.ng@ulster.ac.uk)

This work was supported by ItraMAS Corporation, Malaysia.

ABSTRACT Smart homes and Internet of Things are emerging concepts in modern society, with intelligent lighting being an important part of it. Besides providing visual satisfaction through its color-rendering properties, lighting also has other effects on human well-being. In order to exploit the full potential of a smartly lit home, lighting systems need to be equipped with accurate controllers that can control the spectrum and color characteristics of light in addition to conventional ON–OFF and dimming control. However, current commercial smart lighting products with such capabilities need to employ expensive sensors which are still lacking in terms of closed-loop feedback which is imperative for accurate color control of light-emitting diode (LED)-based luminaires. This paper presents a novel approach that uses the camera available on modern smartphones to perform closed-loop color control for lighting systems in smart homes. The algorithm is able to perform multi-channel mixing for any color and also white light at a desired correlated color temperature with high color-rendering index. This approach proves to be very economical and convenient as no external sensors are required and can be performed using any Android smartphone on a compatible LED-based luminaire.

INDEX TERMS Color control, Internet of Things, LED lighting system, light control, mobile device, multi-channel luminaire, smart homes, smartphone, Zigbee.

I. INTRODUCTION

Light emitting diodes (LEDs) are steadily gaining ground in lighting applications all around the world. It was reported that in the United States alone, the installations of LED products in all lighting applications have more than quadrupled from the year 2014 till 2016 [1]. The U.S. Department of Energy also forecasts that the penetration of LED-based luminaires will increase dramatically to about 86% in general lighting applications by the year 2035 [2]. Many consumers are moving towards LEDs because of its lower power consumption compared to traditional light sources such as halogens and fluorescents. Also, LED-based luminaires offer far greater advantages than just energy savings; they come in various spectral compositions and are also easily controllable, leading to lighting systems which are tunable. Spectrally tunable lights are expected to be the future of lighting, as studies have shown that light is a significant stimulus in influencing the human biological clock [3], [4], where it has been found that the spectral composition of light strongly impacts human physiology and psychology [5], [6]. The attraction of a tunable lighting system is that it can close the gap between artificial lights and natural light, offering huge benefits to human well being. However, with the potential advantages offered by tunable lighting, there are also causes for concern, as tuning could compromise the visual quality of the light. For instance, inappropriately tuned lights could cause objects in the room to have unnatural color rendering, whereby a measure is the Color Rendering Index (CRI) which indicates the difference in the color appearance of objects under the light in comparison with a reference light, with a score of 100 indicating the

best color rendering quality [7]. Hence, there also needs to be significant consideration towards the visual quality in addition to energy efficiency and non-visual benefits. The way forward is to realize tunable lighting systems that consider the aforementioned factors. The wide adoption of such lighting systems require luminaires that are accurately controlled to achieve a desired color point, executed using technologies that are cost effective, user friendly and reliable.

A review of available lighting control systems reveals that existing schemes are inadequate for addressing all these diverse requirements. Within the domain of home automation for energy management, several schemes have been proposed to control home appliances, of which lights are one of them [8]–[11]. However, they are simple on-off or dimming schemes and do not consider the visual nor non-visual effects. Then, there are schemes that provide color control in addition to enhanced energy efficiency [12]–[14], but are open-loop and would not be accurate for color-mixing approaches. This is because the lumen output and spectral power distribution for each colored LED can vary with the *pn* junction temperature [15], [16]. As a result, open-loop schemes cannot achieve accurate control over the light parameters such as its color coordinates ($u'v'$) and correlated color temperature (CCT) which are respectively, the measures of the light color and the color appearance of light as defined by the temperature of a reference (black body) source when it emits the same color as the light.

Closed-loop (feedback) control methods using various models [17], [18] that predict light characteristics such as CCT and $u'v'$ color coordinates based on *pn* junction temperature have been explored to produce white light [19]. However, this method has a major drawback as the *pn* junction temperature feedback does not suffice when there are external light sources such as sunlight entering the room. Other methods include flux feedback [20] or a combination of both flux and junction temperature feedback [15]. In an attempt to perform color control on colors other than white, some research applied RGB color mixing [21], [22] or used spectrophotometers for feedback purposes [23]. But installation of chroma, flux and spectrum sensors is expensive and inconvenient.

One convenient and economical method for efficient color control is to use the smartphone camera as the color sensor in the lighting system in addition to its potential to be used in lux control and energy savings, as initially demonstrated by Tang *et al.* [21], [24]. Past works that use smart-phones for colorimetry have limited features such as recording and analyzing RGB color of a picture [25] and required integration of additional hardware [26]. Given that almost half of the global population own a smartphone nowadays and with the numbers still continuing to grow [27], they are ever more readily-available for such smart applications, eliminating the need to purchase dedicated sensors and hardware. Furthermore, as smartphones become more ubiquitous and powerful, the processing capabilities and sensors on the smartphones may as well be exploited for automation features of an intelligent lighting systems as part of the Internet of Things (IoT) setup in a smart home [28]. However, with the push towards tunable high quality white light which will inevitably employ more than three colors [29], [30], the solution offered in [21] to control RGB LEDs using the color sensor data on a smartphone camera is not sufficient. A gradient descent algorithm is thus proposed in this paper which has the ability to converge to a target color using lights with any number of LED channels. This is achieved by performing computations to determine the shortest path in the $u'v'$ color space in order to achieve the target color in real time. The performances of bi-channel mixing using two white LED channels and tri-channel mixing using RGB channels are also explored as a simpler subset of multi-channel color mixing.

Thus the research proposed in this paper enables the use of the camera available on Android smartphones to capture

TABLE 1. List of symbols and abbreviations.

Symbol	Meaning
p_r, p_g, p_b	red/green/blue responses of camera sensors at point x
$X(t)$	set-point of RGB values
$W(t)$	$u'v'$ color coordinates light room
$G(t)$	spectral reflectances of the surfaces of objects/furniture in room
$H(t)$	smartphone camera reading
$Y(t)$	lighting condition in room
$U(t)$	input to luminaire (via PWM)
$L(t)$	luminaire
$N(t)$	external light sources
x	a point
$e(t)$	error of RGB values between set-point and camera reading
t	time
$E(\lambda)$	spectral power distribution of light source
$S(\lambda, x)$	reflection distribution function at point x
$F_i(\lambda)$	spectral sensitivity function of the $i-th$ sensor
Ω	visible spectral range from $380nmto780$nm
C_{avg}	Average RGB values
M, N	pixel sizes
I_C	average image color
u', v'	color coordinates
u'_{tar}, v'_{tar}	target values of u', v'
u'_{meas}, v'_{meas}	measured values of u', v'
u'_{LED}, v'_{LED}	u', v' values of LEDs
Δ	difference in
LED	light emitting diode
CCT	correlated color temperature
CRI	color rendering index
RGB	red, green, blue
SPD	spectral power density
PI	proportional-integral
PID	proportional-integral-derivative
PWM	pulse-width modulation
CIELUV	International Commission on Illumination color space
ANSI	American National Standards Institute
HSV	Hue Saturation Value

TABLE 2. Color coordinates of the LEDs used in the luminaire.

Channel	CIE 1931 xy		1976 CIELUV	
	x	y	u'	v'
Red (637 nm)	0.7020	0.2975	0.5436	0.5183
Amber (625 nm)	0.6817	0.3178	0.5003	0.5247
Yellow (596 nm)	0.5899	0.4093	0.3505	0.5472
Lime (538 nm)	0.4087	0.5601	0.1836	0.5662
Green (523 nm)	0.1804	0.7281	0.0634	0.5760
Cyan (501 nm)	0.0790	0.5186	0.0348	0.5149
Blue (467 nm)	0.1335	0.0693	0.1498	0.1751
Warm White (2751K)	0.4625	0.4210	0.2596	0.5317
Neutral White (4129K)	0.3763	0.3786	0.2216	0.5018
Cool White (6175K)	0.3173	0.3530	0.1922	0.4813

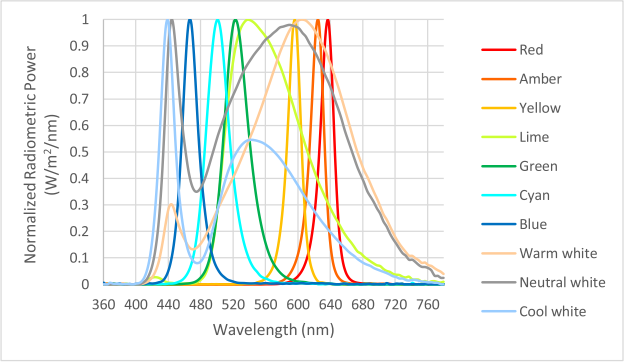

FIGURE 1. Normalized luminaire SPD of the LEDs used.

and to determine the color of the current lighting in the room. By using a custom-built Android Application, closed-loop color control is performed to manipulate the light output from the lights to follow a target set by the user. It is worth noting that the algorithm works using the average color information of an image, and therefore the pixel specifications of all smartphones should be sufficient for this approach to work.

This paper is organized as follows: in Section II, the closed-loop control methodology is described; the design of the algorithm and the pseudocode are presented in Section III; in Section IV, the performance of the algorithm for various lighting conditions through experimentation is discussed, and finally, Section V concludes the paper.

II. LIGHT SPECTRUM CONTROL METHODOLOGY

The luminaire prototype used to test the proposed control algorithm consists of 10 channels, of which 7 are primary colors with different peak wavelengths, whilst the remaining 3 channels are phosphor-converted white LEDs. The peak wavelengths and color coordinates of the LED channels are summarized in Table 2, and their normalized power spectra densities (SPD) are shown in Figure 1. The intensity of each LED channel is controlled using pulse-width modulation (PWM), which is supplied by an Arduino microcontroller on-board the luminaires to the LED driver wirelessly using ZigBee [24]. Each channel can produce 256 different intensities including the off state at a step size of 0.39%.

An Android application was developed to execute the lighting control algorithm. Figure 2 shows the overall schematic

TABLE 3. Specifications of the Oneplus 3 A3000 used to test the color control algorithm.

Operating system	Android 7.1.1 Nougat
CPU	Quad-Core, 2 Processors: 2.15GHz Dual-Core Kryo 1.6GHz Dual-Core Kryo
Memory	6GB LPDDR4 RAM
Primary camera (Back camera)	Sony IMX298 Exmor RS, 16MP
Secondary camera (Front camera)	Sony IMX179 Exmor R, 8MP

block diagram. The user firstly selects the target lighting color, using a color picker (as shown in Figure 3); the algorithm converts that color to a set of $u'v'$ coordinates which is referred to as the target set point $X(t)$. The information of the room lighting condition, $Y(t)$ is captured by the smartphone camera $H(t)$, which is converted to the $u'v'$ color coordinates $W(t)$ of the light in the room. Then the Euclidian distance between $X(t)$ and $W(t)$ is computed to produce the error $e(t)$. The PI controller receives $e(t)$, and considers the color coordinates of the LEDs (obtained from data-sheets), and generates the PWM control signal $U(t)$ to each LED channel in the luminaire $L(t)$, wirelessly using ZigBee. $N(t)$ represents external light sources coming into the room, acting as disturbances or noise in the data measured by the camera. $G(t)$ represents the spectral reflectance of the surfaces of objects and furniture in the room assumed to be Lambertian, whilst $H(t)$ is the response of the smartphone camera used to read the lighting condition $Y(t)$ in the room.

The smartphone used for experimentations and testing of the control algorithm is the OnePlus 3 A3000 with key specifications listed in Table 3. In order to use the camera on the smartphone to perform closed-loop color control on the average light emitted from the luminaire, the following assumptions were made:

1) The smartphone has to be placed at a position and angle such that the secondary camera (front camera) is able to capture the lighting scene of the room.
2) The cameras on the smartphone have been color calibrated during the manufacturing process in the factory itself.
3) The objects and furniture in the room have Lambertian surfaces, where their collective colors average towards gray.

Assumption 3 above corresponds to the Gray World Assumption commonly used in digital photography color constancy algorithms [31]–[34]. The decision to adopt the Gray World Assumption is both valid and logical as there would be many objects of a variety of colors in a typical room.

As such, the response of the smartphone camera to the lighting condition in the room, $H(t)$ at position x in the room is defined by the red, green and blue responses of the camera sensors at the point and can be represented by $[p_r(x), p_g(x), p_b(x)]$ as derived in [35],

$$p_i(x) = \int_{\Omega} E(\lambda)S(\lambda, x)F_i(\lambda)d\lambda \quad \text{for } i = r, g, b \qquad (1)$$

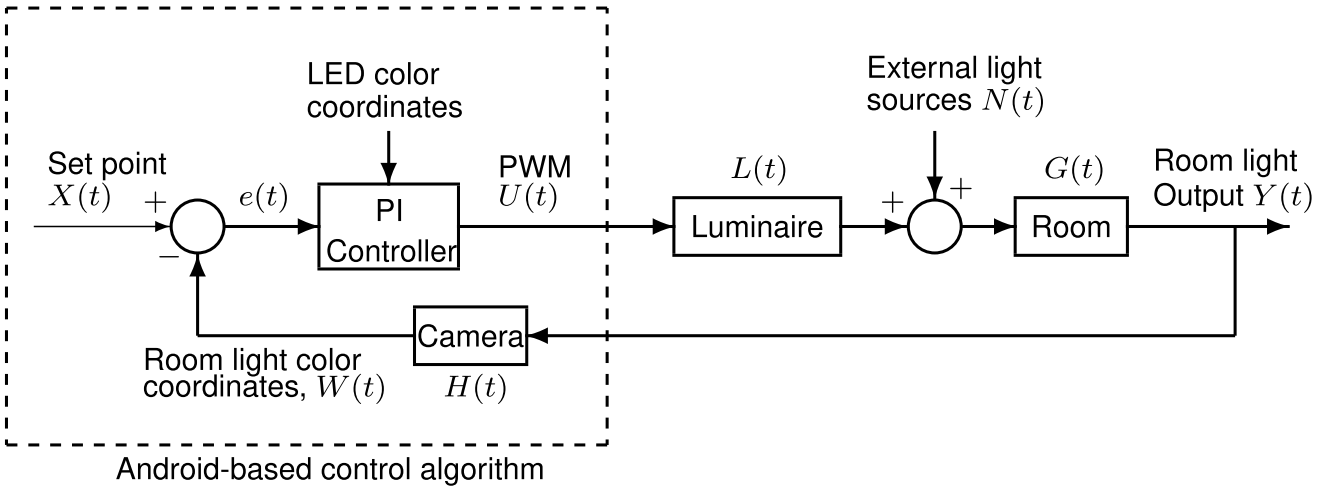

FIGURE 2. Feedback control block diagram for the multi-channel color control.

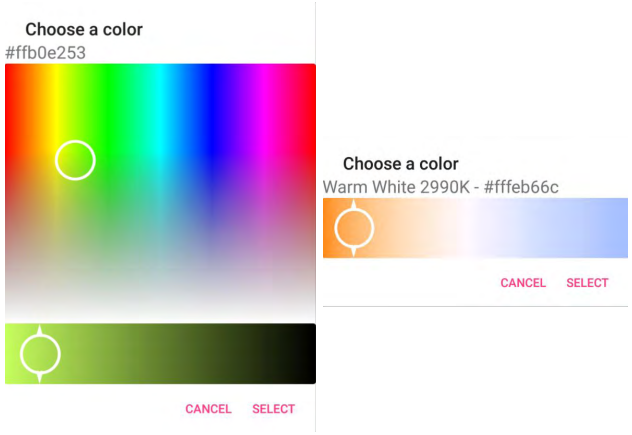

FIGURE 3. Color pickers in the Android application for the user to select the target light color. The screenshot on the left is the HSV (Hue, Saturation, Value) color space while the one on the right is for easier selection of whites along the Planckian Locus. The code to create the color pickers were adapted from a publicly available repository and can be found at `https://github.com/jbruchanov/AndroidColorPicker`.

where, $E(\lambda)$ is the Spectral Power Distribution (SPD) of the light source, $S(\lambda, x)$ the reflectance distribution function at point x, $F_i(\lambda)$ the spectral sensitivity function of the i-th sensor, all expressed as a function of wavelength λ, and Ω represents the visible spectral range from 380nm to 780nm.

With the Gray World Assumption, $S(\lambda, x)$ in (1) would be equal to gray when the whole color scene of the room is averaged. Also, assuming that the RGB sensors in the camera have been calibrated, the computations for $p_i(x)$ from (1) would result in the image captured by the camera representing the color of the light illuminating the room.

The novel multi-channel color control algorithm which is presented in Section III of this paper is a form of the gradient descent algorithm that converges to the target chromaticity as illustrated in Figure 4. The computations are performed in the 1976 CIELUV color space which has a uniform chromaticity scale [36]. For this algorithm to work, the (u', v') coordinates of each LED channel has to be obtained the first time the user runs the system. The algorithm cycles through all LED channels in the luminaire individually while computing the color coordinates using the camera reading as input. The controller algorithm was not specifically tuned to the characteristics of the specific OnePlus 3 A3000 smartphone camera used for validation. This is in line with the assumption that the cameras are calibrated accurately in the factory and also allows validating the accuracy of the algorithm for any smartphone using a similar camera.

The main objective of the algorithm is to develop a fastest and shortest travel path in the CIELUV color space for the color emitted by the LED luminaire to converge to the target color using the closed-loop control design shown in Figure 2. This can be done by tuning the radiometric power output of the LED channels.

The initial resultant color emitted by the LED channels, $Y(t)$ is labeled as point 'Start', whilst the target color, $X(t)$ is set to the point labeled 'Target'. The fact that the color resulting from adding two colors always falls on a line connecting the colors on the chromaticity diagram is used as a basis to iteratively arrive at the final intensities of each LED channel. Figure 4 shows the path that the algorithm took to converge to the target color in a real experiment.

III. DESIGN OF THE MULTI-CHANNEL COLOR CONTROL ALGORITHM

Algorithm 1 shows the pseudocode of the control algorithm which is run in an independent thread to ensure smooth operation of the mobile application. The first step in the algorithm is to scale the size of the image obtained from

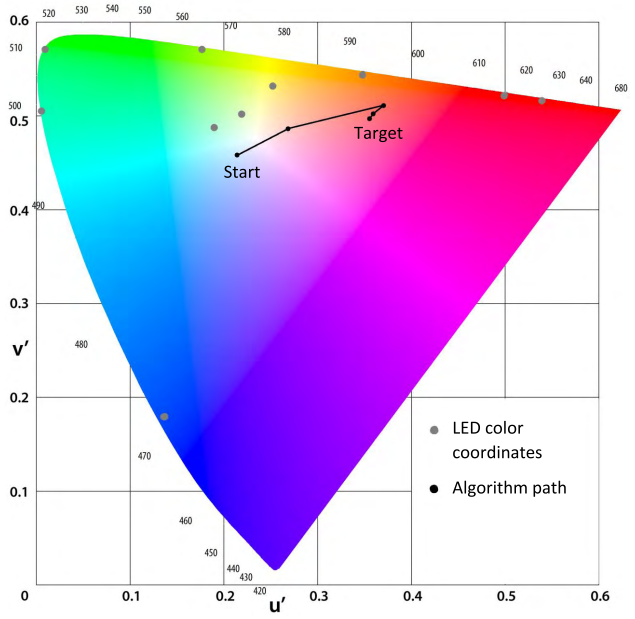

FIGURE 4. The 1976 CIELUV color space with coordinates of the LED channels and an example of an actual path, denoted by a solid black line connecting the 'Start' point to the 'Target' point, that the algorithm took to converge the color emitted by the LED luminaire to the target color.

the camera by reducing the width and height of the image by 10 times respectively, thus resulting in a final image that is 100 times smaller than the original using the Android function `getBitmap()`. Then, the average RGB values in the image are calculated using the following expression

$$C_{avg} = \frac{1}{M \times N} \sum_{x=1}^{M} \sum_{y=1}^{N} I_C(x, y) \tag{2}$$

where C_{avg} represents the average of the red, green, and blue channels, x and y are the indices of the average image color I_C of size M by N pixels.

The RGB values are then used to compute the measured color coordinates (u', v'). The error signal $e(t)$ is computed using the formula

$$\Delta u'v' = \sqrt{(u'_{tar} - u'_{meas})^2 + (v'_{tar} - v'_{meas})^2} \tag{3}$$

where (u'_{tar}, v'_{tar}), (u'_{meas}, v'_{meas}) are the (u', v') coordinates of the target set point color, $X(t)$ and measured color by the camera, $W(t)$, respectively.

A proportional-integral (PI) controller deliberated in [24] is used in the design of the feedback control algorithm in order to achieve zero steady-state error. It was tuned using the well-known Ziegler-Nichols method to calculate the step size for each iteration which provides the algorithm with the capability of adaptive step sizes. The Ziegler-Nichols method is a systematic and practical method of calculating controller gains and has proven successful for designing controllers in various systems. We refer the reader to [37] and [38] for a more detailed description of the method. As a lighting

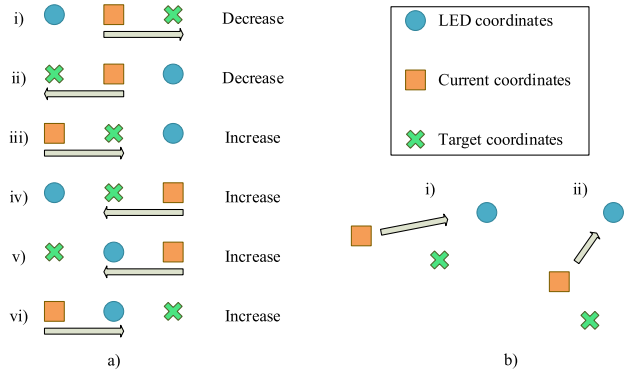

FIGURE 5. Visual aid on how to determine the tuning of the brightness of the LED channel. (a) All possible configurations for a single axis, (b) Example of a 2-axis real world system.

system has slow dynamics and is not susceptible to significant overshoots, a PID controller is not required. In addition, the derivative term could amplify noise in the system.

The next step in the algorithm is to determine if the intensity of each LED channel should be increased or decreased. This is performed by checking the coordinates of the current measured color against those of the target color and the LED channels. Let us consider the operation of only one channel (red) and one coordinate axis (u'). Should the coordinates of the measured color be either lower or higher in value than *both* the LED and target colors, i.e.

$$(u'_{meas} < u'_{tar}) \wedge (u'_{meas} < u'_{LED})$$

or that

$$(u'_{meas} > u'_{tar}) \wedge (u'_{meas} > u'_{LED}),$$

then reducing the intensity of the red LED channel would naturally shift the color closer towards the targeted color, as illustrated in Figure 5a(i–ii). Otherwise, increasing the intensity of the red LED channel would shift the produced color closer towards the LED color, as illustrated in Figure 5a(iii–vi). Lines 15 and 16 in the pseudocode illustrate how this check is carried out.

However, chromaticity being a 2-dimensional space, if it has been determined that the same actions are taken simultaneously for both u' and v' axes, i.e. either increasing or decreasing the intensity, then it is quite straightforward to calculate the new value of the channel. But if increasing the intensity of the channel reduces say the error in the u' axis but increases the error in the v' axis, or vice versa, then the axis with a larger error determines if the intensity of the channel increases or decreases. A visualization of how this could happen is shown in Figure 5b, where reducing the error in the horizontal axis in 5b(i) is a step closer to the target color, but might cause a larger overall error as depicted in 5b(ii).

Finally, the PWM values generated from the Arduino are clipped to a lower bound of 0 and an upper bound of 255, as explained in Line 35. These calculations and operations are done on all channels simultaneously in every feedback loop

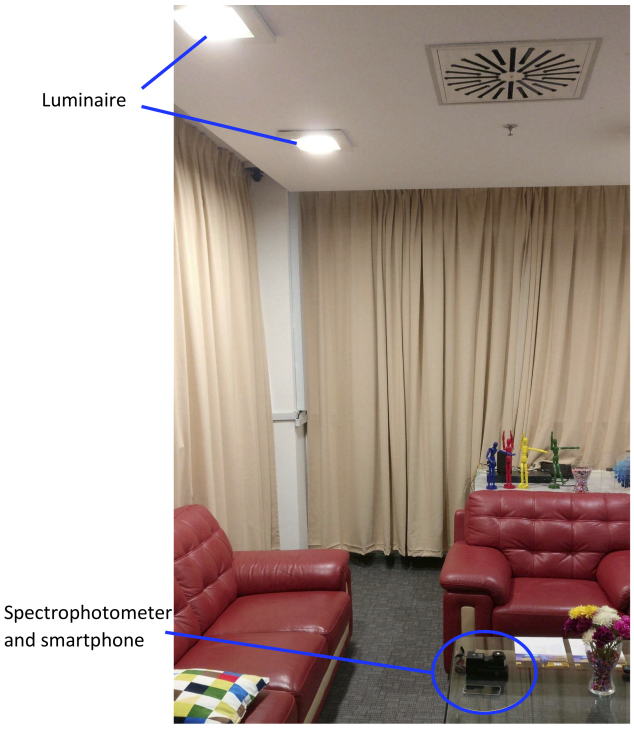

FIGURE 6. The 5.8 m × 3.4 m mock living room used for the experiment.

such that the algorithm converges quickly to the target color. If brightness control of the light output from the luminaire is also required to be done alongside color control, the new PWM values for each channel can be adjusted using Line 34 of the algorithm, where a multiplier is used as the gain to increase or decrease the light intensity of every channel. Additionally, automatic pausing algorithms such as the one implemented in [24] can be integrated into the design to ensure that the user is not deprived of his smartphone use while the feedback control is running.

IV. EXPERIMENTAL RESULTS AND DISCUSSIONS

The experimental system was set up in a mock living room which is a 5.8 m × 3.4 m space, equipped with six wirelessly-controlled and tunable 10-channel research prototype luminaires as shown in Figure 6. The seven channels which are pure-colored LEDs span across the visible wavelength range and can be mixed to obtain white light with a wide range of color properties. The remaining three channels consisting of cool, warm and neutral white phosphor-converted LEDs (PC-LEDs) that emit white light by virtue of a yellow phosphor coating on a blue LED. Properties of white light used to validate the performance of the algorithm are $u'v'$, CCT and CRI.

The smartphone with its secondary camera facing upwards is used to capture the lighting condition, i.e. the RGB values and illuminance of the light incident on the surface where the phone is placed. A Konica Minolta CL-500A illuminance spectrophotometer is placed in close proximity of the smartphone to validate the color-control algorithm. The curtains in the living room allowed the blocking of 100 percent of the external light sources entering the room through the windows. The color control algorithm was tested using two

Algorithm 1 Pseudocode for Multi-Channel Closed-Loop Color Controller (Red Channel of LED Used as an Example)

1: $uTar, vTar \leftarrow$ compute (u'_{tar}, v'_{tar}) ▷ Set point X(t)
2: Get luminaire settings
3: `onSurfaceTextureUpdated()` ▷ Compute RGB data from camera image
4: **if** $(done == true)$ **then** ▷ Check if previous loop is done
5: $done \leftarrow false$
6: $now \leftarrow$ `System.currentTimeMillis()` ▷ Current time
7: $timeChange \leftarrow now - lastTime$
8: $uMeas, vMeas \leftarrow$ compute (u'_{meas}, v'_{meas}) ▷ Compute $u'v'$ color coordinates from RGB data
9: $uDiff \leftarrow uTar - uMeas$
10: $vDiff \leftarrow vTar - vMeas$ ▷ Calculate error $e(t)$
11: $colErr \leftarrow$ compute $\Delta(u', v')$ using $(uDiff, vDiff)$
12: $colErrSum \leftarrow colErrSum + (colErr \times timeChange)$
13: $step \leftarrow (kp \times colErr) + (colErrSum/Ti)$ ▷ PI controller
14: **for** Each channel **do** ▷ Red channel used as example
15: $uu \leftarrow (uDiff < 0) == ((uRed - uMeas) < 0)$
16: $vv \leftarrow (vDiff < 0) == ((vRed - vMeas) < 0)$ ▷ Compare measured (u', v') with Target (u', v')
17: **if** $(uu \wedge vv)$ **then**
18: $red \leftarrow red + step$ ▷ Increase intensity
19: **else if** $(uu == true)$ **then**
20: **if** $(|uRed - uMeas| > |vRed - vMeas|)$ **then**
21: $red \leftarrow red + step$
22: **else**
23: $red \leftarrow red - step$ ▷ Decrease intensity
24: **end if**
25: **else if** $(vv == true)$ **then**
26: **if** $(|uRed - uMeas| < |vRed - vMeas|)$ **then**
27: $red \leftarrow red + step$
28: **else**
29: $red \leftarrow red - step$
30: **end if**
31: **else**
32: $red \leftarrow red - step$
33: **end if**
34: $red \leftarrow red \times gain$ ▷ Generate PWM signal $U(t)$
35: $red \leftarrow min(max(red, 0), 255)$ ▷ Keep value of channel within [0, 255]
36: **end for**
37: $lastTime \leftarrow now$ ▷ For $timeChange$ calculation
38: $done \leftarrow true$ ▷ Feedback loop is done
39: **end if**
▷ Repeat until emitted color converges to target color

TABLE 4. Summary of experimental results using bi-color mixing.

Experiment	Average $\Delta u'v'$	CCT range	Average absolute CCT error	Average CRI
Warm white & cool white	0.0103	2700K to 5600K	4.45%	77.7
Cool white & yellow	0.0089	2700K to 5600K	3.62%	59

TABLE 5. Summary of experimental results using multi-channel mixing.

Experiment	Average $\Delta u'v'$	Average absolute CCT error	Average CRI
7 primaries to produce white light	0.0124	10.59%	82.76
10 channels to produce white light	0.0129	9.42%	94
7 primaries to produce non-white light	0.0168	–	–
10 channels to produce non-white light	0.0107	–	–

approaches;

(i) Bi-channel mixing employing two channels
(ii) Multi-channel mixing using pure-colored LED channels

The reasons for using both the approaches are given in the following subsections.

A. BI-CHANNEL MIXING

Although industry players are slowly adopting multi-channel lighting systems for their proposed benefits, luminaires with two instead of many LED channels is an attractive option to save cost and complexity of design and manufacturing. The developed algorithm is thus studied for the case of 2 channels to produce white light for general lighting purposes to determine the feasibility of such a simplified system. Consequently, Algorithm 1 was improvised to run on only 2 LED channels in order to produce 18 different white lights with CCT ranging from 2700K to 5600K. These values were chosen such that the error signal $\Delta u'v'$ across all white lights would not exceed 0.01. Although more relaxed than the ANSI standard $\Delta u'v'$ tolerance of 0.006 [39], this ensures that the algorithm is able to compute the control signals for the luminaire to produce the whole range of CCT with equal steps for the case of two channels.

This experiment was conducted with two different LED pairings

(i) Warm white with cool white, and
(ii) Cool white with yellow

The choice of LED pairings is based on their positions on the CIE chromaticity diagram giving the highest possibility of tuning the resultant white along the Planckian Locus which is most preferred. The summary of the experimental results is tabulated in Table 4.

To measure the accuracy of the color produced by the luminaires, the color selected by the user from the color picker in the mobile application as shown in Figure 3 was converted into the 1976 CIELUV (u', v') coordinates. They were then compared with the readings from the Konica Minolta CL-500A illuminance spectrophotometer. The CCT and CRI of the light produced were also obtained from the spectrophotometer.

From the results in Table 4, the $\Delta u'v'$ of the two cases have an average of 0.0103 and 0.0089 across the range of CCTs generated corresponding to about a 9-step MacAdam ellipse [36]. It can be seen that the color quality is superior for warm white with cool white mixture due to the wider spectrum of warm white compared to yellow LED. Since the color accuracy is similar in both cases, the warm white with cool white combination is preferred and could be implemented in the consumer market with precise CCT control.

B. MULTI-CHANNEL MIXING

The color control algorithm was then tested using the following scenarios:

(i) Seven primary colors to produce white light
(ii) Ten LED channels to produce white light
(iii) Seven primary colors to produce a colored light
(iv) Ten LED channels to produce a colored light

The test cases for all scenarios were conducted 25 times to produce CCT ranging from 2500K to 8000K with each test using randomly selected colors with various hues and saturations for scenarios (iii) and (iv). The results of these tests are tabulated in Table 5.

For this case, the feedback algorithm was programmed to stop when it detects that the color difference $\Delta u'v'$ less than 0.003, a more stringent value compared to bi-channel mixing. This target was met for every chosen color detected by the smartphone camera. However, it can be seen from the spectrophotometer readings that the measured color difference of the actual light generated is higher and at the same level as the bi-channel light mixture. The color difference can be further reduced if the calibration of the smartphone camera is customized.

The average CRI however, was considerably high at 82.76 for seven-channel mixing with pure-color LEDs and 94 for ten-channel mixing. By optimizing the choice of LED primaries in the luminaire, the number of LED channels required to produce a larger color gamut and high CRI light can be further reduced.

In terms of timing performance, each step in the closed-loop control consists of the following tasks: obtaining readings from the camera, performing calculations for the next step in the iteration, sending new PWM values to the luminaires, and waiting for feedback response from the sensor.

The average time taken by each iteration was approximately 658ms, with the algorithm taking about 10 iterations to converge the output of the luminaires from a random color to the target color. This is equivalent to about 6–7s. This rate of convergence by the algorithm is reasonable as well as acceptable in real-world applications as it allows for a much richer and more comfortable user experience compared to sudden changes in the color outputs. Furthermore, disturbances from external light sources such as natural light entering the room would happen on a much larger time scale compared to the convergent time of the algorithm.

V. CONCLUSION

This paper has presented a novel approach for color control of a multi-channel LED lighting system in a smart home environment using the camera found on most modern Android smartphones as the main feedback sensor. The algorithm is able to optimize the output spectrum of the luminaires to produce a light with tunable CCT, accurate color and high color rendering index. A closed-loop feedback control system helps maintain robustness towards external disturbances from other light sources such as sunlight coming in through the windows.The algorithm is able to work at reasonable accuracy with potential improvement if customized camera calibration data is used. The proposed method of using the smartphone as both a sensor and a processing unit proves to be very economical and convenient as no additional sensors are needed to be installed. Future work can include among other features, mood lighting based on user preference and the replication of a lighting scene that a user has captured on the smartphone from a different location.

REFERENCES

[1] J. Penning, S. Schober, K. Stober, and M. Yamada, "Adoption of light-emitting diodes in common lighting applications," U.S. Dept. Energy, Washington, DC, USA, Tech. Rep. DOE/EE-1016, 2017.
[2] J. Penning, K. Stober, V. Taylor, and M. Yamada, "Energy savings forecast of solid-state lighting in general illumination applications," U.S. Dept. Energy, Washington, DC, USA, Tech. Rep. DOE/EE-1467, 2016.
[3] G. C. Brainard *et al.*, "Action spectrum for melatonin regulation in humans: Evidence for a novel circadian photoreceptor," *J. Neurosci.*, vol. 21, no. 16, pp. 6405–6412, 2001.
[4] K. Thapan, J. Arendt, and D. J. Skene, "An action spectrum for melatonin suppression: Evidence for a novel non-rod, non-cone photoreceptor system in humans," *J. Physiol.*, vol. 535, no. 1, pp. 261–267, 2001.
[5] R. J. Lucas *et al.*, "Measuring and using light in the melanopsin age," *Trends Neurosci.*, vol. 37, no. 1, pp. 1–9, 2014.
[6] T. A. LeGates, D. C. Fernandez, and S. Hattar, "Light as a central modulator of circadian rhythms, sleep and affect," *Nature Rev. Neurosci.*, vol. 15, no. 7, pp. 443–454, 2014.
[7] "Method of measuring and specifying colour rendering properties of light sources," Int. Commission Lighting, Vienna, Austria, Tech. Rep. CIE 13.3, 1995.
[8] F. J. Bellido-Outeirino, J. M. Flores-Arias, M. Linan-Reyes, E. J. Palacios-Garcia, and J. J. Luna-Rodriguez, "Wireless sensor network and stochastic models for household power management," *IEEE Trans. Consum. Electron.*, vol. 59, no. 3, pp. 483–491, Aug. 2013.
[9] Y.-T. Lee, W.-H. Hsiao, C.-M. Huang, and T. C. Seng-Cho, "An integrated cloud-based smart home management system with community hierarchy," *IEEE Trans. Consum. Electron.*, vol. 62, no. 1, pp. 1–9, Feb. 2016.
[10] M. Aliberti, "Green networking in home and building automation systems through power state switching," *IEEE Trans. Consum. Electron.*, vol. 57, no. 2, pp. 445–452, May 2011.
[11] C.-H. Lien, Y.-W. Bai, and M.-B. Lin, "Remote-controllable power outlet system for home power management," *IEEE Trans. Consum. Electron.*, vol. 53, no. 4, pp. 1634–1641, Nov. 2007.
[12] P. K. Maiti and B. Roy, "Evaluation of a light controller for a LED-based dynamic light source," *Lighting Res. Technol.*, vol. 50, no. 4, pp. 571–582, 2018.
[13] H.-J. An, K.-W. Kim, M.-H. Ryu, H.-Y. Oh, N.-G. Kim, and K.-J. Park, "Smartphone-driven low-power light-emitting device," *J. Healthcare Eng.*, vol. 2017, Apr. 2017, Art. no. 5076965.
[14] T. Wu *et al.*, "Improvements of mesopic luminance for light-emitting-diode-based outdoor light sources via tuning scotopic/photopic ratios," *Opt. Express*, vol. 25, no. 5, pp. 4887–4897, 2017.
[15] S. Muthu, F. J. P. Schuurmans, and M. D. Pashley, "Red, green, and blue LEDs for white light illumination," *IEEE J. Sel. Topics Quantum Electron.*, vol. 8, no. 2, pp. 333–338, Mar. 2002.
[16] F.-C. Wang, C.-W. Tang, and B.-J. Huang, "Multivariable robust control for a red–green–blue LED lighting system," *IEEE Trans. Power Electron.*, vol. 25, no. 2, pp. 417–428, Feb. 2010.
[17] L. Lohaus, E. Leicht, S. Dietrich, R. Wunderlich, and S. Heinen, "Advanced color control for multicolor LED illumination systems with parametric optimization," in *Proc. 39th Annu. Conf. IEEE Ind. Electron. Soc. (IECON)*, Nov. 2013, pp. 3305–3310.
[18] S.-P. Ying, H.-K. Fu, H.-H. Hsieh, and H.-W. Kuo, "The modeling of two phosphors in conversion white-light LED," *IEEE Trans. Electron Devices*, vol. 64, no. 3, pp. 1088–1093, Mar. 2017.
[19] H.-T. Chen, S.-C. Tan, and S. Y. Hui, "Nonlinear dimming and correlated color temperature control of bicolor white LED systems," *IEEE Trans. Power Electron.*, vol. 30, no. 12, pp. 6934–6947, Dec. 2015.
[20] A. T. L. Lee, H. Chen, S.-C. Tan, and S. Y. Hui, "Precise dimming and color control of LED systems based on color mixing," *IEEE Trans. Power Electron.*, vol. 31, no. 1, pp. 65–80, Jan. 2016.
[21] S. J. W. Tang, K. Y. Ng, V. Kalavally, and J. Parkkinen, "Closed-loop color control of an RGB luminaire using sensors onboard a mobile computing system," in *Proc. IEEE Student Conf. Res. Develop. (SCOReD)*, Dec. 2016, pp. 1–5.
[22] M. Ashibe, M. Miki, and T. Hiroyasu, "Distributed optimization algorithm for lighting color control using chroma sensors," in *Proc. IEEE Int. Conf. Syst., Man (SMC)*, Oct. 2008, pp. 174–178.
[23] I. Chew, V. Kalavally, C. P. Tan, and J. Parkkinen, "A spectrally tunable smart led lighting system with closed-loop control," *IEEE Sensors J.*, vol. 16, no. 11, pp. 4452–4459, Jun. 2016.
[24] S. Tang, V. Kalavally, K. Y. Ng, and J. Parkkinen, "Development of a prototype smart home intelligent lighting control architecture using sensors onboard a mobile computing system," *Energy Buildings*, vol. 138, pp. 368–376, Mar. 2017.
[25] N. Moonrungsee, S. Pencharеeb, and J. Jakmunee, "Colorimetric analyzer based on mobile phone camera for determination of available phosphorus in soil," *Talanta*, vol. 136, pp. 204–209, May 2015.
[26] J. Miettinen, J. B. Martinkauppi, and P. Suopajärvi, "3DS-colorimeter based on a mobile phone camera for industrial applications," *Proc. SPIE, Sensors, Cameras, Syst. Ind. Sci. Appl. XIV*, vol. 8659, p. 86590M, Feb. 2013.
[27] J. Poushter, "Smartphone ownership and Internet usage continues to climb in emerging economies," *Pew Res. Center*, vol. 22, pp. 1–44, Feb. 2016.
[28] R. Piyare, "Internet of Things: Ubiquitous home control and monitoring system using android based smart phone," *Int. J. Internet Things*, vol. 2, no. 1, pp. 5–11, 2013.
[29] D. Lin, P. Zhong, and G. He, "Color temperature tunable white LED cluster with color rendering index above 98," *IEEE Photon. Technol. Lett.*, vol. 29, no. 12, pp. 1050–1053, Jun. 15, 2017.
[30] C.-H. Chiang, S.-J. Gong, T.-S. Zhan, K.-C. Cheng, and S.-Y. Chu, "White light-emitting diodes with high color rendering index and tunable color temperature fabricated using separated phosphor layer structure," *IEEE Electron Device Lett.*, vol. 37, no. 7, pp. 898–901, Jul. 2016.
[31] D. Lee and K. N. Plataniotis, "A taxonomy of color constancy and invariance algorithm," in *Advances in Low-Level Color Image Processing*. Dordrecht, The Netherlands: Springer, 2014, pp. 55–94.
[32] G. D. Finlayson and E. Trezzi, "Shades of gray and colour constancy," in *Proc. Color Imag. Conf.*, Jan. 2004, pp. 37–41.
[33] J. van de Weijer, T. Gevers, and A. Gijsenij, "Edge-based color constancy," *IEEE Trans. Image Process.*, vol. 16, no. 9, pp. 2207–2214, Sep. 2007.
[34] G. Buchsbaum, "A spatial processor model for object colour perception," *J. Franklin Inst.*, vol. 310, no. 1, pp. 1–26, Jul. 1980.

[35] M. Lecca, "On the von Kries model: Estimation, dependence on light and device, and applications," in *Advances in Low-Level Color Image Processing*. Dordrecht, The Netherlands: Springer, 2014, pp. 95–135.
[36] Y. Ohno and P. Blattner, "Chromaticity difference specification for light sources," Int. Commission Illumination, Vienna, Austria, Tech. Rep. CIE TN 001:2014, 2014.
[37] J. G. Ziegler and N. B. Nichols, "Optimum settings for automatic controllers," *J. Dyn. Syst., Meas., Control*, vol. 115, pp. 220–222, Jun. 1993.
[38] C. C. Hang, K. J. Åström, and W. K. Ho, "Refinements of the Ziegler–Nichols tuning formula," *IEE Proc. D (Control Theory Appl.)*, vol. 138, no. 2, pp. 111–118, 1991.
[39] *ENERGY STAR Program Requirements for Integral LED Lamps*, ENERGY STAR, New York, NY, USA, 2010.

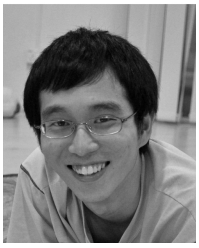

SAMUEL JIA WEI TANG received the B.Eng. degree (Hons.) and the Master of Engineering Science (Research) degree from Monash University in 2013 and 2017, respectively. He was with Monash University, where he involved in the Project Mobile Control of Intelligent Lighting Systems in collaboration with ItraMAS Corporation, Malaysia. Before that, he was involved in Real-Time Lane Detection and Front-End Collision Avoidance System on a Mobile Computing Platform for his final-year project. During his infant research career, he has presented his findings in IEEE conferences and a publication with an international peer-reviewed journal.

VINEETHA KALAVALLY received the Ph.D. degree from Monash University, Australia, in 2012. She is currently a Senior Lecturer with the School of Engineering, Monash University Malaysia, where she is the Head of the Intelligent Lighting Laboratory. Her research interests include optical amplifiers, diverse applications of solid-state lighting, visual and non-visual quality of light, as well as visible light communications.

KOK YEW NG is currently a Lecturer with the School of Engineering, Ulster University, U.K., where he also conducts research with the Nanotechnology and Integrated Bioengineering Centre.

He received the B.Eng. degree (Hons.) and the Ph.D. degree in fault diagnosis from Monash University in 2006 and 2009, respectively. From 2014 to 2015, he was a Post-Doctoral Researcher with the Division of Vehicular Systems, Linköping University, Sweden, where he focused on the advanced fault diagnosis schemes using model-based and data-driven methods on vehicular engines with Volvo Car Corporation. He is currently an Adjunct Researcher with the Research Group. He is also an Adjunct Senior Research Fellow with the School of Engineering, Monash University Malaysia. His research interests are fault diagnosis, vehicular systems, signal processing and data analytics for anomaly detection and classification, as well as machine learning.

CHEE PIN TAN received the B.Eng. degree (Hons.) and the Ph.D. degree from Leicester University, Leicester, U.K., in 1998 and 2002, respectively. He was a Lecturer with the School of Engineering, Monash University Malaysia, in 2002, where he was subsequently promoted to a Senior Lecturer in 2008 and an Associate Professor in 2013. He has authored over 50 internationally peer-reviewed research articles, including a book on fault reconstruction. His research interests include robust fault estimation and observers.

JUSSI PARKKINEN is currently a Professor Emeritus with the University of Eastern Finland, Finland.

He received the M.Sc. degree in medical physics and the Ph.D. degree in mathematics from the University of Kuopio, Finland, in 1982 and 1989, respectively. From 1989 to 1990, he was a Visiting Researcher with The University of Iowa, IA, USA. During 1991–2011, he was a Professor in Computer Science, the Head of Department, and the Dean in three different universities in Finland. From 2011 to 2014, he was a Professor and the Head of Electrical and Computer Systems Engineering Discipline with Monash University Malaysia, where he has been an Adjunct Professor since 2014. He specializes in spectral color science, lighting research, and pattern recognition. He is a fellow of the International Association of Pattern Recognition. He received the Raymond C. Bowman Award by IS&T in 2013. He was the Chairman of the CIE TC8-07 Technical Committee on Multispectral Imaging from 2004 to 2008.